Optical and Quantum Electronics (2024) 56:468
https://doi.org/10.1007/s11082-023-06112-w

Broadband sum-frequency conversion of multiline Q-switched CO laser emission under its double-pass through AR-coated $ZnGeP_2$ crystal

I. O. Kinyaevskiy[1,2] · Yu. M. Klimachev[1] · M. V. Ionin[1] · A. M. Sagitova[1] · M. M. Zinovev[2,3] · N. N. Yudin[2,3] · A. A. Ionin[1]

Received: 21 June 2023 / Accepted: 13 December 2023 / Published online: 27 January 2024

Abstract
Broadband sum-frequency conversion of multiline (~60 spectral lines within ~5–6 μm wavelength interval) Q-switched CO laser emission in an AR-coated $ZnGeP_2$ crystal was experimentally studied by application of both single-pass and double-pass optical schemes. The maximum conversion efficiency in the double-pass scheme reached ~10% that is 2.5 times higher than one obtained in the same optical scheme with an uncoated $ZnGeP_2$. The spectrum control of frequency converted radiation by changing angles of incident and reversed CO laser beams in the $ZnGeP_2$ crystal was implemented within the wavelength range from 2.52 μm up to 2.92 μm. The maximum spectrum width of 0.35 μm was obtained with the double-pass scheme when the angle of the laser beam incident on the crystal and the angle of the deflected reversed laser beam were −4.0° and 1.0°, respectively, the spectral bandwidth being three times broader than one obtained with the single-pass scheme.

Keywords Broadband mid-IR laser · Sum-frequency generation · CO laser · AR-coated $ZnGeP_2$ · Double-pass scheme

1 Introduction

A lot of the strongest fundamental vibrational absorption bands for various gaseous substances including hazardous (toxic, drug and explosive) ones are in the mid-IR range. Therefore, this range is often called as the "molecular-fingerprint region" (Picqué and Hänsch 2019). Accordingly, to solve a number of problems (for example, environmental monitoring and air control of a working area, analysis of processed gases and gas mixtures

✉ Yu. M. Klimachev
klimachevym@lebedev.ru

[1] Lebedev Physical Institute of the Russian Academy of Sciences, 53 Leninskiy Ave., Moscow, Russia 119991

[2] National Research Tomsk State University, 36 Lenin Ave, Tomsk, Russia 634050

[3] LOC LLC, 28 Vysotsky Str., Tomsk, Russia 634040

composition, detection of leaks in main gas and oil pipelines), the development of broadband mid-IR laser sources is required.

One of the most efficient amongst such laser sources is a CO laser. The cascade mechanism of its lasing leads to the fact that the CO laser has the highest efficiency among gas-discharge lasers, in the multiline mode reaching 50% for fundamental ro-vibrational transitions (Ionin 2007) and 16% for overtone ro-vibrational transitions (Ionin et al. 2006). This laser can generate on the large number (hundreds) of spectral lines in a broad wavelength range (Ionin 2007). For the fundamental vibrational bands, this range spans from 4.6 μm (McCord et al. 2000) up to 8.7 μm (Ionin et al. 2017a), and for overtone vibrational bands, from 2.5 μm up to 4.2 μm (Ionin et al. 2010). In addition, many spectral lines of the CO laser are within the spectral intervals of low atmospheric absorption, i.e. within the atmospheric transparency windows (Ionin et al. 2013, 2022a).

However, a number of problems require radiation with wavelengths that go beyond CO laser spectral bands. One of the methods for expanding and enriching the spectrum of a CO laser is frequency conversion of its emission in nonlinear crystals.

Due to the latter, the Gas Laser Laboratory of P. N. Lebedev Physical Institute of RAS has implemented broadband sum-frequency generation (SFG) in several nonlinear crystals: $ZnGeP_2$ (Ionin et al. 2018), $AgGaSe_2$ (Budilova et al. 2016), $BaGa_2GeSe_6$, GaSe (Badikov et al. 2018), and $PbIn_6Te_{10}$ (Ionin et al. 2016) with external conversion efficiency of 2.5%, 0.6%, 0.5%, 0.15% and 0.01%, respectively. It should be noted that these experiments were carried out with the same Q-switched CO laser and under the same conditions of focusing into a nonlinear crystal (by a lens with the focal length $F = 20$ cm). Therefore, after comparing the obtained results, we can claim that just the $ZnGeP_2$ nonlinear crystal is the most efficient for this type of conversion. The CO laser SFG efficiency enhancement in nonlinear crystals $ZnGeP_2$ is possible by several procedures.

Firstly, an increase of the SFG efficiency is possible due to a sharper focusing (Andreev et al. 2013). In this case, the maximum external efficiency of the SFG was achieved by focusing with a lens with $F = 11.5$ cm, which made it possible to operate at laser intensities on the crystal surface close to the optical damage threshold (for a $ZnGeP_2$ crystal 78 MW/cm^2 (Dmitriev et al. 1999)). At the moment, the external efficiency of the SFG is 3.4% that, taking into account Fresnel reflection losses from uncoated crystal faces, corresponds to the internal efficiency of 6.5%. However, this result was obtained nearly to the optical damage threshold of a $ZnGeP_2$ crystal.

Secondly, it is potentially possible to increase the SFG efficiency by using an intracavity SFG scheme (Ionin et al. 2022b). In our intracavity SFG experiments, the efficiency of 2.9% (Ionin et al. 2022b) was obtained at laser intensity on the crystal surface of 0.9 MW/cm^2 that is 85 times lower than the optical damage threshold for a $ZnGeP_2$ crystal. Calculations performed in (Ionin et al. 2022b) demonstrated following results: if the intracavity laser intensity on the crystal surface increases up to 10 MW/cm^2, (for example, due to an additional intracavity focusing lens (Petukhov et al. 2001)), there is some potential to achieve intracavity SFG efficiency up to 25%.

Thirdly, conversion efficiency can be increased by an application of a double-pass scheme. The double-pass scheme provided about 30% higher efficiency of CO laser SFG in a $ZnGeP_2$ crystal as compared to a traditional single-pass one (Kinyaevskiy et al. 2023), while the spectral bandwidth of frequency converted radiation was the same. Moreover, a feasibility of slight spectral bandwidth extension by a variation of a reverse beam direction was demonstrated for the double-pass scheme. It must be noted that the double-pass SFG scheme automatically solves the problem of SFG radiation walk-off effect (Bhar et al. 1990) in contrast to an optical scheme with two crystal samples (Antipov et al. 2017).

The fourth option for increasing the conversion efficiency is application of a nonlinear crystal AR-coating which is the objective of the given paper research. This research became possible due to the development of new broadband multirange AR-coatings (Zinovev et al. 2022) for the $ZnGeP_2$ crystal with the high optical damage threshold both in the CO laser spectral range (5–7 μm) and in the sum-frequencies range (2.5–3.5 μm). Thus, in this paper the broadband SFG of multiline Q-switched CO laser radiation was studied in AR-coated $ZnGeP_2$ crystal samples under single-pass and double-pass schemes.

2 Experimental setup

The experiments were carried out with a low-pressure cryogenic Q-switched CO laser pumped by a DC discharge. Figure 1 shows the general optical scheme of the experiments. The active medium of the CO laser was mixture $He:N_2:CO:Air = 140:11:2:1$ at gas pressure of 7.7 Torr. The laser cavity was formed by high reflecting spherical mirror 1 (the radius of curvature $r = 9$ m) and a flat output mirror with ~ 25% transmittance. A high reflecting rotating mirror was placed inside the laser cavity, which provided the laser operation in the Q-switched mode with repetition rate of ~ 60–130 Hz.

The CO laser spectrum consisted of ~ 60 spectral lines in the wavelength range from 4.9 to 6.2 μm, its maximum being near the wavelength of 5.2 μm (see Fig. 2). The CO laser total peak power integrated over its spectrum was up to ~ 4.5 kW. The peak power of the CO laser individual spectral lines in Fig. 2 was calibrated to the integrated peak power.

To control the CO laser average output power, a part of its emission (~ 6%) was directed into Ophir-3A power meter by a BaF_2 plate and spherical mirror 2 ($r = 1$ m). The second BaF_2 plate was used to control the laser pulse temporal shape with PEMI-10.6 photodetector (time resolution 1 ns).

In the experiment, both the single-pass and double-pass SFG schemes were used. In the first case, the main part (~ 94%) of the CO laser emission was focused into a nonlinear AR-coated $ZnGeP_2$ crystal with a CaF_2 lens (the focal distance $F = 200$ mm). After the crystal, the radiation was directed by spherical mirror 3 ($r = 50$ cm) to the SFG characteristics measuring system.

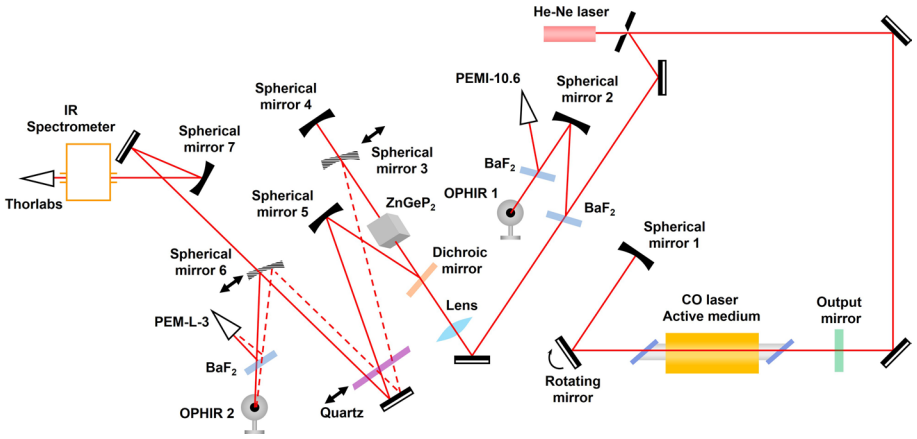

Fig. 1 General optical scheme of the experiment

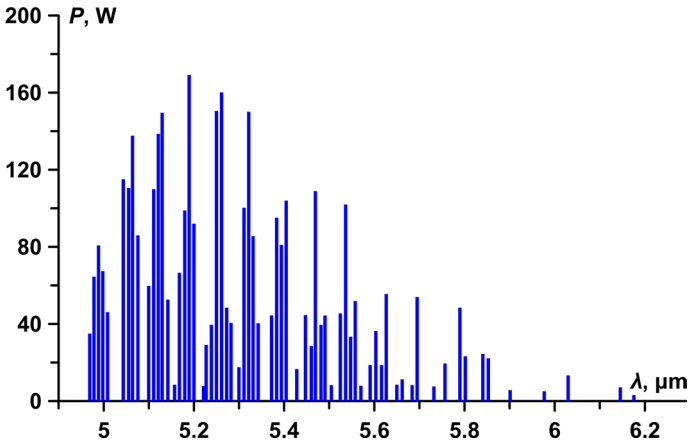

Fig. 2 The CO laser spectrum

In the second case, the main part of the radiation was focused into the $ZnGeP_2$ crystal with the same lens ($F=200$ mm) through a flat dichroic mirror (reflection coefficient $R\sim99\%$ in the SFG wavelength range and $\sim10\%$ in the CO laser wavelength range). After the crystal, the CO laser beam was reversed into the crystal by spherical mirror 4 ($r=30$ cm) either straight back (the deflecting angle $\beta=0°$) or deflected by a small angle in the horizontal plane ($\beta=1.0°$), (see Fig. 3). In Fig. 3, the angle α denotes the CO laser beam angle of incidence on the nonlinear crystal during the first pass.

The SFG radiation obtained as a result of two passes of the CO laser emission through the $ZnGeP_2$ crystal and a part of the CO laser radiation were reflected by the dichroic mirror to spherical mirror 5 ($r=60$ cm), and, then, directed to the SFG characteristics measuring system. A quartz plate was used as a spectral filter to separate SFG radiation from the CO laser emission. The following SFG characteristics were measured: a temporal pulse shape, average power, and spectrum. With spherical mirror 6, the SFG radiation was

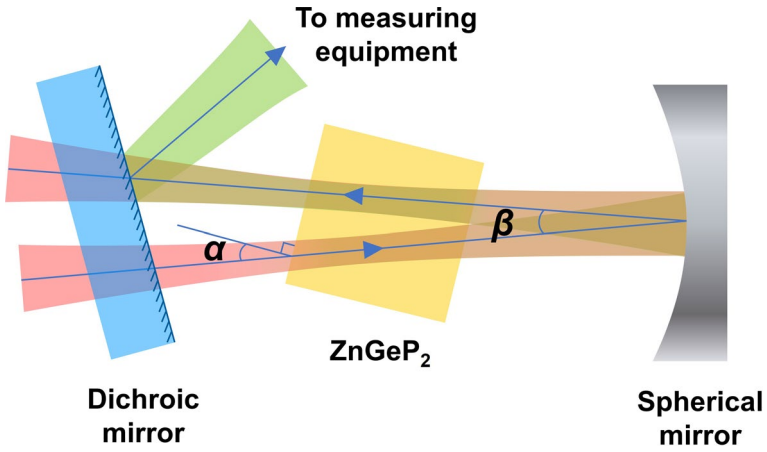

Fig. 3 Scheme of a double pass through the AR-coated $ZnGeP_2$ crystal: α is the incidence angle of the laser beam on the crystal; β is the deflecting angle of the laser beam in the horizontal plane

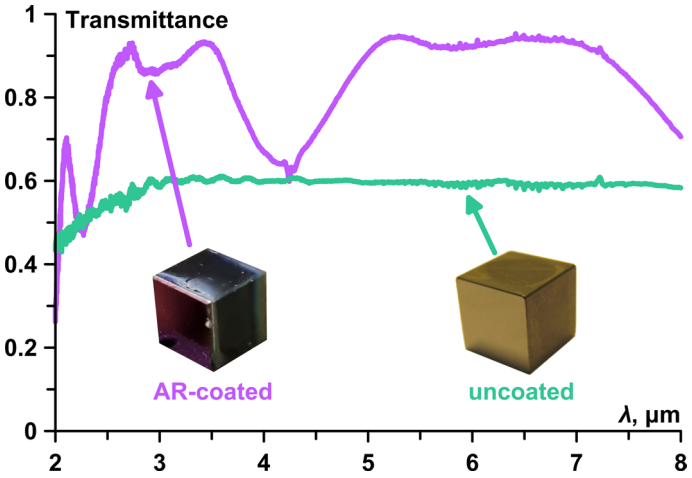

Fig. 4 Transmittance and photos of AR-coated and uncoated samples of the nonlinear $ZnGeP_2$ crystal

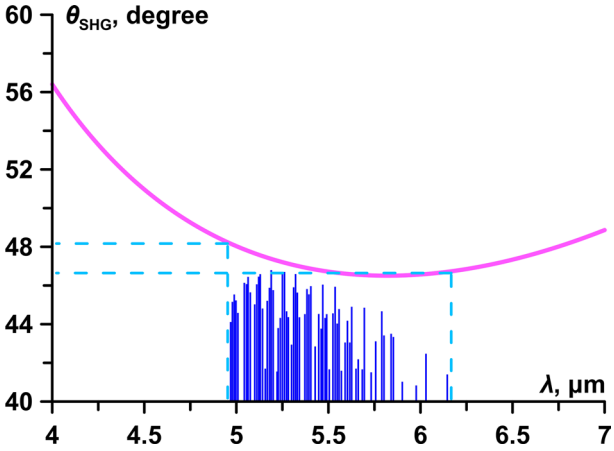

Fig. 5 Dependence of a phase-matching angle for second harmonic generation (a particular case of SFG) by type e + e → o in $ZnGeP_2$ crystal on a pump (CO laser) wavelength and CO multiline laser spectrum in a logarithmic scale

focused onto Ophir-3A power meter to measure the average SFG power. To determine the pulse shape, it was directed onto PEM-L-3 photodetector (time resolution 0.5 ns) with a plane-parallel BaF_2 plate. To measure the SFG spectrum, its radiation was directed to the input slit of IR spectrometer IKS-31, LOMO Ltd (spectral resolution ~ 1 nm). Photodetector Thorlabs PDA20H was installed at the IR spectrometer output slit. A He–Ne laser beam was used to align the optical scheme.

The experimental sample of nonlinear $ZnGeP_2$ crystal of $8 \times 8 \times 8$ mm^3 volume was grown and AR-coated on both sides at «Laboratory of optical crystals LLC, Russia». Transmittance of the sample was ~ 85–90% within the SFG wavelength range and ~ 92–95% within the CO laser wavelength range (see Fig. 4).

Figure 5 demonstrates a dependence of a phase-matching angle for second harmonic generation (a particular case of SFG) by type e + e → o in $ZnGeP_2$ crystal on a pump (CO laser) wavelength. Also, CO laser spectrum in a logarithmic scale transferred from Fig. 2 is indicated in Fig. 5. Since the CO laser spectrum is located near the dependence minimum,

the noncritical spectral phase-matching for SFG of multiline CO-laser radiation takes place (Andreev et al. 2013). Thus, broadband SFG with a great number of frequency conversion lines is possible in the $ZnGeP_2$ under the crystal fixed angle.

3 Experimental results and discussion

3.1 Single-pass SFG scheme

3.1.1 SFG time characteristics

Figure 6 shows the temporal pulse shapes of the CO laser and SFG pulses at various mirror rotation frequencies (Q-switching frequencies). These curves are the waveforms of the CO laser pulse incident on the crystal and the SFG pulse coming out of the crystal representing the time dependence of the respective powers. The peak power of the CO laser $P_{\text{peak}}^{\text{CO}}$, i.e. the maximum radiation power per pulse, increases with Q-switching frequency rise reaching its maximum at frequency $f = 86$ Hz, and then begins to decline. This decline is associated with a sharp decrease in the pulse energy, because as the mirror rotation speed increases, the time the resonator remains in the adjusted state declines and lasing does not have time to be developed effectively. A shape of the CO laser pulse changed from "triangular" to "Gaussian" with the Q-switching frequency increase.

Measured FWHM duration of the CO laser pulse ($t_{1/2}^{\text{CO}}$) and the SFG pulse ($t_{1/2}^{\text{SFG}}$) at different Q-switching frequencies (f) are presented in Fig. 7. They had a general trend of declining with Q-switching frequency increase. But CO laser and SFG pulse durations were the same within measurement error bars at low $f \sim 60$ Hz and notably different at high $f \sim 130$ Hz.

To explain this fact, we should consider the SFG theory taking into account a peculiarity of CO lasing time behavior on different spectral lines. The SFG power P_3 and the conversion efficiency K can be represented by expressions (1, 2), see, for example, the Handbook of Nonlinear Optical Crystals (Dmitriev et al. 1999):

$$P_3 = \frac{8\pi^2 d_{\text{eff}}^2 L^2 P_1 P_2}{\varepsilon_0 c n_1 n_2 n_3 \lambda_3^2 A} \operatorname{sinc}^2\left(\frac{|\Delta k| L_{\text{eff}}}{2}\right), \tag{1}$$

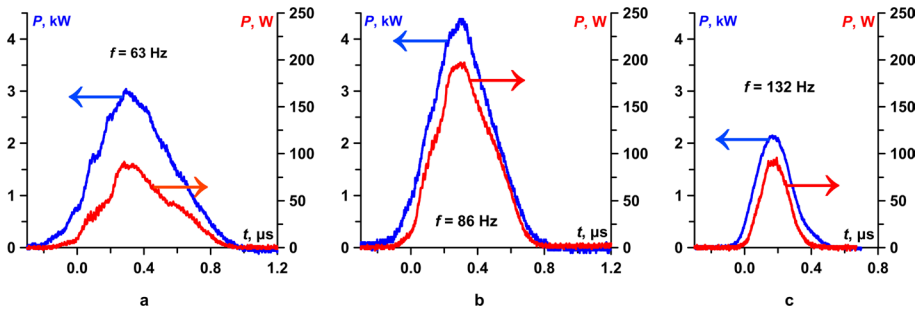

Fig. 6 CO laser (left axes) and SFG (right axes) temporal pulse shapes at different mirror rotation frequencies: **a** 63 Hz, **b** 86 Hz, **c** 132 Hz

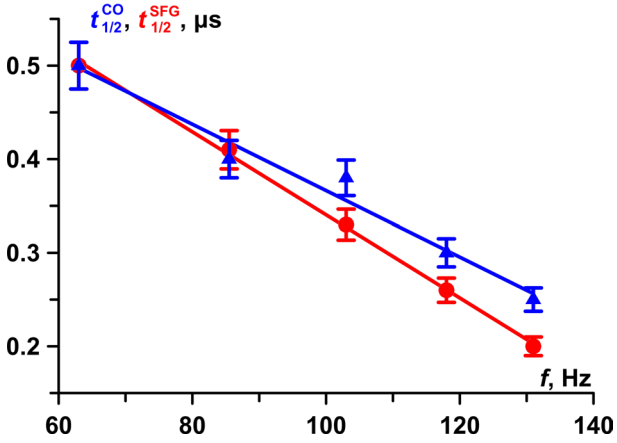

Fig. 7 FWHM duration of the CO laser (triangles) and SFG (circles) pulses versus Q-switching frequency f

$$K = \frac{8\pi^2 d_{\text{eff}}^2 L^2 P_1}{\varepsilon_0 c n_1 n_2 n_3 \lambda_3^2 A} \operatorname{sinc}^2\left(\frac{|\Delta k| L_{\text{eff}}}{2}\right), \tag{2}$$

where d_{eff} is effective nonlinear coefficient; n_i are the refractive indices at λ_i; λ_3 is SFG wavelength; ε_0 is vacuum permittivity; P_1 и P_2 are power of CO laser lines; P_3 is SFG power; Δk is wavelength mismatch; L_{eff} is effective crystal length; A is cross-sectional area of the laser beam; c is speed of light in vacuum.

According to expression (1), the SFG power is proportional to the product of the pump lines peak power. Therefore, at exact (ideal) temporal matching of the pump pulses (as well as for the second harmonic generation), the SFG pulse duration is $\sqrt{2}$ shorter than the pump pulse duration. In our case, this is clearly not so, especially, at low Q-switching frequency (see Fig. 7). This is due to the fact that the CO lasing time behavior on individual ro-vibrational transitions is not the same even in the Q-switching mode (Ionin et al. 2017b). Such a behavior resulted in the "triangular" shape of the integrated over their spectrum CO laser and SFG pulses (see Fig. 6a) with similar duration at the low Q-switching frequency. At the high Q-switching frequency of 130 Hz the SFG pulse duration was 1.25 times shorter than that of the CO laser (tending to the $\sqrt{2}$ ratio) because lasing dynamics on different CO laser transitions has a better temporal matching which was demonstrated in (Ionin et al. 2017b).

3.1.2 SFG power and conversion efficiency

Figure 8a demonstrates the dependences of the CO laser (P_{CO}) and SFG (P_{SFG}) average power on the Q-switching frequency f. Figure 8b shows the CO laser peak power ($P^{\text{CO}}_{\text{peak}}$) and SFG peak power ($P^{\text{SFG}}_{\text{peak}}$) on the frequency f. Figure 8c demonstrates the average-power conversion efficiency ($K_{\text{av}} = P_{\text{SFG}}/P_{\text{CO}}$) and peak-power conversion efficiency ($K_{\text{peak}} = P^{\text{SFG}}_{\text{peak}}/P^{\text{CO}}_{\text{peak}}$) as functions of the frequency f.

The maximum values of both the average power and peak power of the CO laser emission incident on the crystal (it will be called just the CO laser emission or beam further on) and SFG radiation, as well as the average power and peak power conversion efficiency, were achieved at frequency $f = 86$ Hz. It can be seen that after passing the

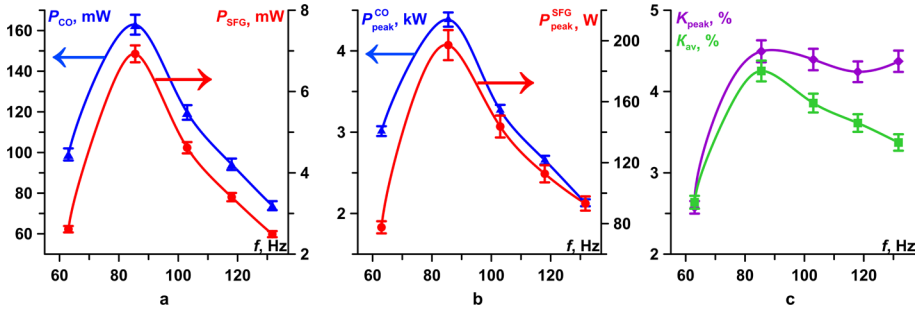

Fig. 8 **a** Average power of the CO laser radiation incident on the crystal P_{CO} and the SFG P_{SFG} average power versus Q-switching frequency f; **b** peak power of the CO laser P^{CO}_{peak} and SFG radiation P^{SFG}_{peak} versus f; **c** average conversion efficiency K_{av} and peak conversion efficiency K_{peak} versus f

maximum, the average power conversion efficiency decreases from $K_{av} = 4.3\%$ down to $K_{av} = 3.4\%$, while the peak power conversion efficiency changes just a little remaining in the range of 4.25–4.5%. This can be explained by the fact that the SFG peak power does not go down as sharply as that of CO laser due to a better SFG conversion caused by the better temporal matching of CO laser pulses on different ro-vibrational transitions.

3.1.3 SFG spectrum

Figure 9 shows the SFG spectrum for the case of a single-pass obtained under SFG conversion efficiency $K_{av} = 3.7 \pm 0.3\%$ (the incidence angle of the CO laser beam $\alpha = 0°$). It contained ~ 40 detected spectral lines in the wavelength range from 2.52 μm up to 2.65 μm with the maximum of the SFG spectrum at $\lambda \sim 2.58$ μm. The spectrum bandwidth was ~ 0.1 μm at 0.1 level.

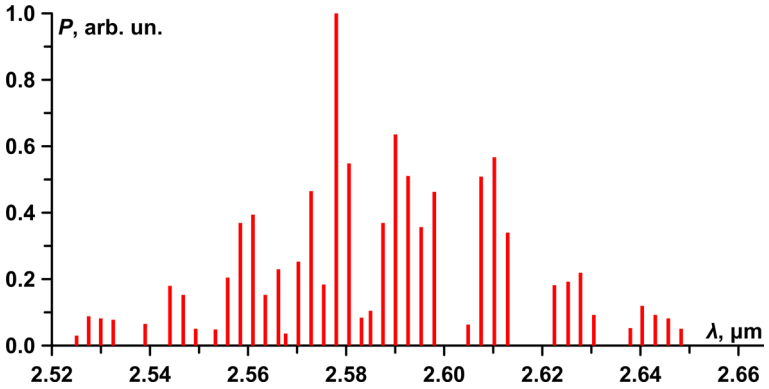

Fig. 9 SFG spectrum observed in the single-pass scheme

3.2 Double-pass SFG scheme

3.2.1 SFG average power and conversion efficiency

To increase SFG efficiency the double-pass scheme was implemented. Figure 10 demonstrates the dependences of the SFG average power and the average power conversion efficiency K_{av} on the CO laser average power for one and two passes through the $ZnGeP_2$ nonlinear crystal ($f = 103$ Hz, $\alpha = 0°$, $\beta = 0°$). The CO laser average power was controlled by a variable attenuator based on a mid-IR polarizer. In both cases, the SFG average power grew up quadratically, and the conversion efficiency K_{av} grew up linearly with the CO laser average power increase, as it was supposed by the expressions (1) and (2). Thus, these expressions adequately describe the experiment even in the case of broadband SFG of multiline CO laser under noncritical spectral phase-matching conditions.

Following the obtained dependencies, we calculated the gain factor for the SFG in the second pass through the $ZnGeP_2$ sample:

$$G = P_{SFG}^{\text{second pass}} / P_{SFG}^{\text{one pass}}, \tag{3}$$

where $P_{SFG}^{\text{second pass}}$ — SFG power in the second pass through the $ZnGeP_2$ sample, $P_{SFG}^{\text{one pass}}$ — SFG power in the one pass through the $ZnGeP_2$ sample. Figure 11 demonstrates the gain factor G for the SFG in the second pass through the $ZnGeP_2$ crystal. The gain factor was from 2 to 3.5 depending on the CO laser average power. The reason for the gain factor to be higher than 2 means that the second pass provided not just linear addition to the single-pass SFG power, but did provide the nonlinear increase of SFG power. However, the gain factor went down with the CO laser power enhancement. At the moment, a reason for the SFG gain factor to go down in the second pass is yet unclear for us; this decrease may be related with frequency conversion saturation for the strongest SFG spectral lines.

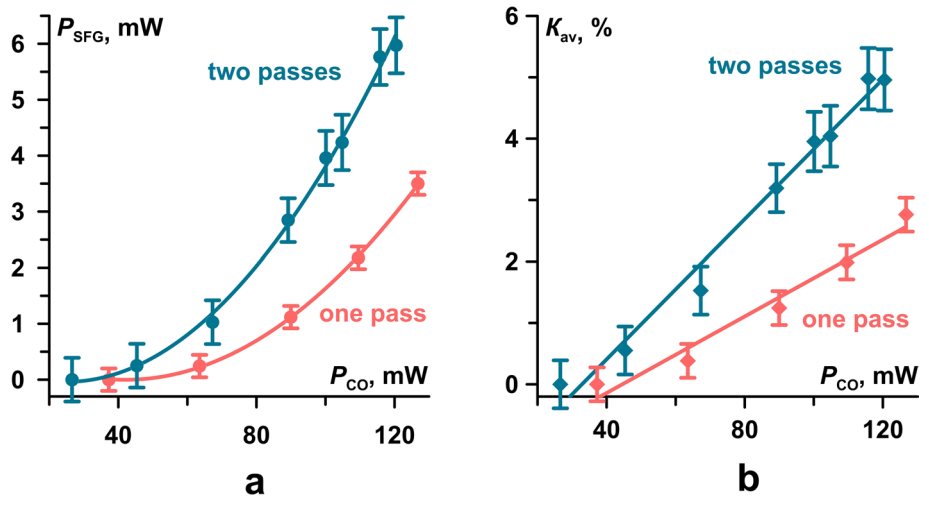

Fig. 10 Dependencies of the SFG average power P_{SFG} **a** and the conversion efficiency K_{av} **b** on the CO laser average power for one and two passes

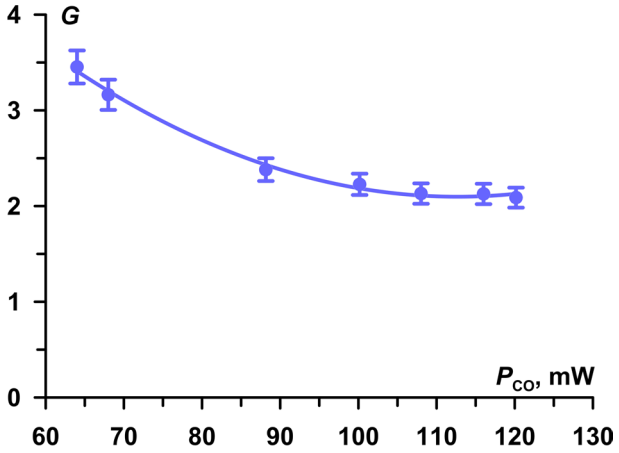

Fig. 11 Gain factor of the SFG radiation in the second pass versus CO laser average power

In the next experiments, we studied an effect of CO laser beam incidence angle (α) on the SFG power, conversion efficiency, and SFG spectrum. This angle was changed by rotating the nonlinear crystal. Figure 12 shows the dependences of the average SFG power (P_{SFG}) and conversion efficiency K_{av} on the angle of incidence α (two passes, $\beta = 0°$). It can be seen that the maxima of both P_{SFG} and K_{av} take place at the angle of incidence ~ 0.7°. The maximum SFG average power was 13.9 ± 0.7 mW, that corresponded to $K_{av} = 9.7 \pm 0.5\%$. For the normal incidence, the conversion efficiency was slightly lower, $K_{av} = 8.2 \pm 0.5\%$. This indicates that the crystal cut angle does not perfectly match the optimal one for the broadband SFG. It can be noted that P_{SFG} and K_{av} are above the level of 0.5 relative to their maxima in a wide range of incidence angles — from –3 to 0 degrees. This fact allows us to hope that under the intracavity conversion of CO laser emission in the AR-coated nonlinear $ZnGeP_2$ crystal, it is possible to tune the SFG spectrum not only by changing the crystal temperature (Ionin et al. 2016), but also by rotating the crystal relative to the cavity axis.

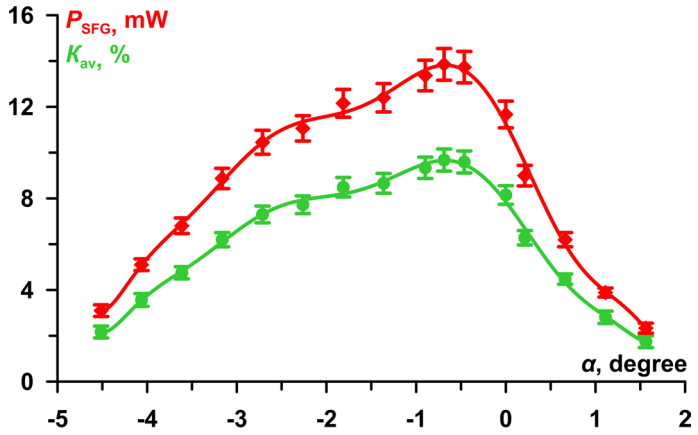

Fig. 12 SFG average power P_{SFG} (rhombs) and conversion efficiency K_{av} (circles) versus the CO laser beam angle of incidence α for two passes ($f = 106$ Hz, $\beta = 0°$)

3.2.2 SFG spectrum

Figures 13(a–c) show the SFG spectra in the case of two passes through the crystal with the reverse laser beam directed exactly backwards (the deflecting angle $\beta = 0°$). For the angles of incidence $\alpha = 0°$ and $\alpha = -1.0°$, it contained ~ 80 spectral lines in the wavelength range from 2.52 μm up to 2.75 μm. For $\alpha = -1.4°$, it contained ~ 130 spectral lines in the wavelength range from 2.52 μm up to 2.8 μm, the maximum of the SFG spectrum being shifted to 2.65 μm.

Figures 13(d–f) demonstrate the SFG spectra for the case of two passes, while the laser beam traveled back at the deflecting angle $\beta = 1.0°$, i.e. the phase-matching angle in the $ZnGeP_2$ crystal was slightly different in the second pass. The results show for the spectrum at the angle of incidence $\alpha = 0°$ to be the narrowest one, the number of SFG lines being ~ 55 in the wavelength range from 2.52 μm to 2.66 μm. Spectral width on level 0.1 in this case was 0.11 μm. The narrowest SFG spectrum obtained under these conditions was due to the fact that phase-matching conditions were shifted to the

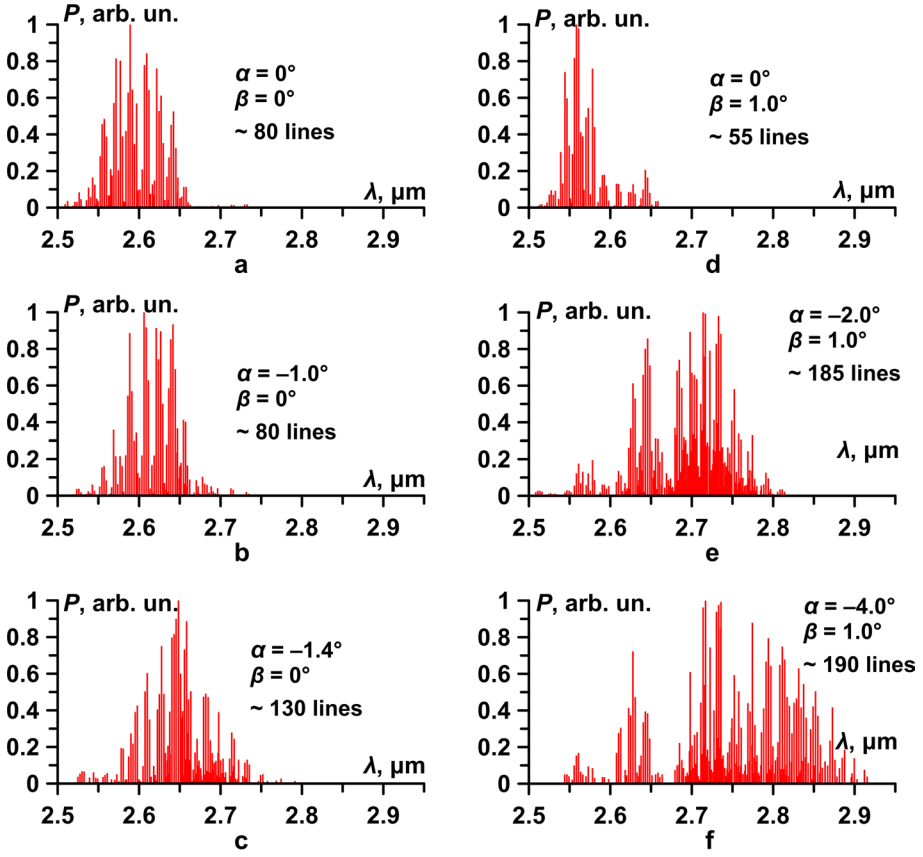

Fig. 13 SFG spectrum at different angles of incidence (α) of the CO laser beam on the $ZnGeP_2$ crystal. Second pass back at the deflecting angle $\beta = 0°$, **a** $\alpha = 0°$, **b** $\alpha = -1.0°$, **c** $\alpha = -1.4°$; second pass back at the deflecting angle $\beta = 1.0°$, **d** $\alpha = 0°$, **e** $\alpha = -2.0°$, **f** $\alpha = -4.0°$

shortwave edge of the CO laser spectrum with higher steep slope in the SFG dependence in Fig. 5, and a small number of CO laser lines (near 5.1 μm) were converted.

At the angle of incidence $\alpha = -2.0°$, the spectrum expanded to the long wavelength region up to 2.82 μm, the number of SFG spectral lines increasing up to ~ 185. At the angle of incidence $\alpha = -4.0°$, the spectrum expanded up to 2.92 μm, the number of SFG spectral lines being ~ 190. Spectral width on level 0.1 in this case was 0.35 μm that was three times higher than one for the normal incidence ($\alpha = 0°$, $\beta = 0°$) and for the single-pass scheme (see Fig. 9). Thus, this geometry ($\alpha = -4°$, $\beta = 1°$) provided the best overlapping of phase-matching conditions of the first and second passes through the crystal to obtain the widest SFG spectrum involving almost all CO laser spectral lines.

4 Conclusions

A broadband sum-frequency conversion of multiline Q-switched CO laser emission under its single-pass and double-pass through an AR-coated $ZnGeP_2$ crystal was experimentally studied, CO laser radiation being focused back into the crystal by a spherical mirror in the latter case. The maximum conversion efficiency in the double-pass scheme came up to ~ 10% that was 2.5 times higher than one in an uncoated nonlinear $ZnGeP_2$ crystal for the same optical scheme (Kinyaevskiy et al. 2023). The control over the SFG spectrum was demonstrated by changing the CO laser radiation angle of incidence on the $ZnGeP_2$ crystal within the wavelength range from 2.52 μm up to 2.92 μm. The broadest SFG spectrum was observed with the double-pass scheme when the CO laser beam was not directed straight back, but was deflected by the angle of 1.0° and passed through the crystal, the angle of incidence of the laser beam on the crystal being –4.0°. The number of SFG spectral lines came up to ~ 190. The SFG spectrum width on level 0.1 was three times broader as compared to the narrowest spectrum obtained in our experiments (the deflecting and incidence angles 1.0° and 0°, respectively).

The research was partially supported from the Russian Science Foundation grant № 22–22-20103, https://rscf.ru/project/22-22-20103/ and Tomsk region administration.

Authors contributions IOK, YMK and AMS made experiments YMK, MVI and AMS processed the results of experiments, prepared figures The nonlinear $ZnGeP_2$ crystal was grown and AR-coated by MMZ and NNY; IOK, YMK and MVI wrote the main manuscript text IOK, YMK and AAI edited the manuscript text.

Funding The research was supported by the Russian Science Foundation grant № 22-22-20103 and Tomsk region administration.

Declarations

Competing interests The authors declare no competing interests.

References

Andreev, Y.M., Ionin, A.A., Kinyaevsky, I.O., Klimachev, Y.M., Kozlov, A.Y., Kotkov, A.A., Lanskii, G.V., Shaiduko, A.V.: Broadband carbon monoxide laser system operating in the wavelength range

of 2.5–8.3 μm. Quantum Electron. **43**(2), 139–143 (2013). https://doi.org/10.1070/QE2013v043n02ABEH014978

Antipov, O.L., Eranov, I.D., Kositsyn, R.I.: 10-W mid-IR optical parametric oscillators based on $ZnGeP_2$ elements pumped by a fibre-laser-pumped Ho: YAG Laser. Exp. Numer. Study. Quantum Electron. **47**(7), 601–606 (2017). https://doi.org/10.1070/QEL16366

Badikov, D.V., Badikov, V.V., Ionin, A.A., Kinyaevskiy, I.O., Klimachev, Y.M., Kotkov, A.A., Mitin, K.V., Mokrousova, D.V., Mojaeva, V.A.: Sum-frequency generation of Q-switched CO laser radiation in $BaGa_2GeSe_6$ and GaSe nonlinear crystals. Opt. Quant. Electron. **50**(6), 243 (2018). https://doi.org/10.1007/s11082-018-1514-0

Bhar, G.C., Chatterjee, U., Datta, P.: Enhancement of second harmonic generation by double-pass configuration in barium borate. Appl. Phys. B **51**(5), 317–319 (1990). https://doi.org/10.1007/BF00348966

Budilova, O.V., Ionin, A.A., Kinyaevskiy, I.O., Klimachev, Y.M., Kotkov, A.A., Kozlov, A.Y., Lanskii, G.V.: Broadband two-stage frequency conversion of CO laser in $AgGaSe_2$ crystal. Opt. Lett. **41**(4), 777–780 (2016). https://doi.org/10.1364/OL.41.000777

Dmitriev, V.G., Gurzadyan, G.G., Nikogosyan, D.N.: Optics of Nonlinear Crystals. In: Siegman, A.E. (ed.) Handbook of Nonlinear Optical Crystals, pp. 3–66. Springer Series in Optical Sciences **(64)**, Springer, Berlin, Heidelberg (1999). https://doi.org/10.1007/978-3-540-46793-9_2

Ionin, A.A.: Electric Discharge CO Lasers. In: Endo, M., Walter, R.F. (eds.) Gas Lasers, pp. 201–237. CRC Press, Boca Raton (2007)

Ionin, A.A., Klimachev, Y.M., Kozlov, A.Y., Kotkov, A.A., Kurnosov, A.K., Napartovich, A.P., Rulev, O.A., Seleznev, L.V., Sinitsyn, D.V., Hager, G.D., Shnyrev, S.L.: A pulsed overtone CO laser with efficiency of 16%. Quantum Electron. **36**(12), 1153–1154 (2006). https://doi.org/10.1070/QE2006v036n12ABEH013330

Ionin, A.A., Kurnosov, A.K., Napartovich, A.P., Seleznev, L.V.: Lasers on overtone transitions of carbon monoxide molecule. Laser Phys. **20**(1), 144–186 (2010). https://doi.org/10.1134/S1054660X09180042

Ionin, A.A., Klimachev, Yu.M., Kozlov, AYu., Kotkov, A.A., Matvienko, G.G., Romanovskii, O.A., Kharchenko, O.V., Yakovlev, S.V.: Application of an overtone CO laser for remote gas analysis of the atmosphere. Atmos. Oceanic Opt. **26**(1), 68–73 (2013). https://doi.org/10.1134/S1024856013010090

Ionin, A.A., Kinyaevskiy, I.O., Klimachev, Y.M., Kotkov, A.A., Badikov, V.V., Mitin, K.V.: Frequency conversion of molecular gas lasers in $PbIn_6Te_{10}$ crystal within mid-IR range. Opt. Lett. **41**(10), 2390–2393 (2016). https://doi.org/10.1364/OL.41.002390

Ionin, A.A., Kinyaevskiy, I.O., Klimachev, Yu.M., Mozhaeva, V.A., Andreev, Yu.M.: Three-stage frequency conversion of sub-microsecond multiline CO laser pulse in a single $ZnGeP_2$ crystal. Opt. Lett. **43**(13), 3184–3187 (2018). https://doi.org/10.1364/OL.43.003184

Ionin, A.A., Kinyaevskiy, I.O., Klimachev, Y.M., Kotkov, A.A., Kozlov, A.Y.: Frequency tunable CO laser operating on the highest vibrational transition with wavelength of 8.7 μm. Opt. Lett. **42**(3), 498–501 (2017a). https://doi.org/10.1364/OL.42.000498

Ionin, A.A., Kinyaevskiy, I.O., Klimachev, Y.M., Kryuchkov, D.S., Sagitova, A.M., Sunchugasheva, E.S.: Spectral characteristics of multi-line Q-switched CO laser radiation frequency converted in $ZnGeP_2$. Appl. Phys. B **123**(9), 234 (2017b). https://doi.org/10.1007/s00340-017-6812-x

Ionin, A.A., Kinyaevskiy, I.O., Kotkov, A.A., Sinitsyn, D.V., Andreev, Y.M.: Compact radio frequency discharge-pumped slab CO laser system with a zinc germanium phosphide ($ZnGeP_2$) sum-frequency generator for remote sensing of the atmosphere. Appl. Spectrosc. **76**(12), 1504–1512 (2022a). https://doi.org/10.1177/00037028221119837

Ionin, A.A., Kinyaevskiy, I.O., Klimachev, Y.M., Kotkov, A.A., Kozlov, A.Y., Sagitova, A.M., Sinitsyn, D.V., Rulev, O.A.: Double-range (λ = 2.6–2.9 and 4.9–6.0 μm) slab RF discharge CO laser system with intracavity frequency conversion in temperature-controlled $ZnGeP_2$ crystal. Opt. Laser Technol. **148**, 107777 (2022b). https://doi.org/10.1016/j.optlastec.2021.107777

Kinyaevskiy, I.O., Klimachev, Yu.M., Ionin, M.V., Sagitova, A.M., Zinovev, M.M., Ionin, A.A.: Broadband sum-frequency conversion of multiline Q-switched CO laser emission under its double-pass through uncoated $ZnGeP_2$ crystal. Infrared Phys. Technol. **132**, 104740 (2023). https://doi.org/10.1016/j.infrared.2023.104740

McCord, J.E., Ionin, A.A., Phipps, S.P., Crowell, P.G., Lampson, A.I., McIver, J.K., Brown, A.J., Hager, G.D.: Frequency-tunable optically pumped carbon monoxide laser. IEEE J. Quantum Electron. **36**(9), 1041–1052 (2000). https://doi.org/10.1109/3.863956

Petukhov, V.O., Gorobets, V.A., Tochitsky, S.Y., Kozlov, K.V.: Efficient intracavity frequency doubling of CO_2 laser in nonlinear crystals. In: Proc. SPIE 4351, Laser Optics 2000: High-Power Gas Lasers (2001). https://doi.org/10.1117/12.417705

Picqué, N., Hänsch, T.W.: Frequency comb spectroscopy. Nat. Photon. **13**(3), 146–157 (2019). https://doi.org/10.1038/s41566-018-0347-5

Zinovev, M., Yudin, N.N., Kinyaevskiy, I., Podzyvalov, S., Kuznetsov, V., Slyunko, E., Baalbaki, H., Vlasov, D.: Multispectral anti-reflection coatings based on YbF_3/ZnS materials on $ZnGeP_2$ substrate by the IBS method for Mid-IR laser applications. Crystals **12**(10), 1408 (2022). https://doi.org/10.3390/cryst12101408